JETIR.ORG ISSN: 2349-5162 | ESTD Year : 2014 | Monthly Issue
JOURNAL OF EMERGING TECHNOLOGIES AND INNOVATIVE RESEARCH (JETIR)
An International Scholarly Open Access, Peer-reviewed, Refereed Journal

DESIGN OF A DEEP LEARNING-BASED MODEL TO ENHANCE AND RECONSTRUCT THE ENVIRONMENTAL IMAGES

Shikha Sain, Dr.Monika Saxena

PhD Scholar, Associate Professor

Banasthali Vidyapith

Abstract: The goal of this work is to create a deep learning-based model for enhancing and reconstructing environmental pictures. Using cutting-edge deep learning methods, a new model architecture is suggested to increase the quality and authenticity of environmental photographs. The model is trained and tested on a dataset of various environmental situations, including landscapes, urban regions, and natural ecosystems. Performance is evaluated using common criteria like as accuracy, precision, recall, and F1-score. The suggested model's accuracy, precision, recall, and F1-score were all 98.71%, indicating its usefulness. When compared to current approaches, such as DenseNet and Standard-CNN, the suggested model outperforms them all, highlighting its potential to develop picture enhancement and reconstruction techniques in environmental monitoring and analysis**.**

IndexTerms **- Cross-Domain CNN, DenseNet, Standard-CNN, Hyperspectral imaging.**

I. INTRODUCTION

A class of machine learning methods known as "deep learning" makes use of multilayered neural networks to automatically interpret signals or data. These deep neural networks are made up of multiple layers of artificial neurons, and each layer usually includes an activation function or nonlinear operation, which, combined, can simulate any function [1]. Deep networks have demonstrated remarkable efficacy in a diverse range of applications, including natural language processing[2], picture classification [3], and playing games like Go [4]. Since their initial proposal in the 1940s [5], neural networks have been continuously developed over many years. Decades of study have gone into developing several types of deep networks, including convolutional neural networks (CNNs) [6] and long short-term memory (LSTM) [7]. CNNs have shown good results in processing, manipulating, and classifying images, partly because of their shift-invariance quality. In the 1980s and 1990s, CNNs started to be employed for tasks like document reading [8]. But recently, a "perfect storm" of hardware (such as more powerful GPUs), data accessibility, and efficient software [9] has made deep learning—more especially, CNNs—a viable solution for challenging issues across numerous scientific domains, chief among them computer vision. One of the most fundamental issues in machine vision, image categorization is a task that has been included in many of these challenges. It is widely employed in numerous sectors [10].

In addition to classification, deep learning offers a plethora of intriguing prospects for resolving traditional inverse problems in imaging, including pixel super-resolution (also known as geometrical super-resolution), denoising, and deblurring. Imaging inverse problems have a long and rich history, encompassing many concepts relevant to deep learning. These include dictionary learning example-based super- resolution approaches [11] and deconvolution algorithms [12] that necessitate a precise understanding of the picture degradation model. Expanding the literature on topics that are traditionally not classified as inverse problems, such as style transfer [13] and image-to-image transformation [14], among others, has been made possible by deep learning.

The primary goal of this research is to pioneer a transformative deep learning model that not only enhances and reconstructs images of the environment but also incorporates spectroscopic data into the imaging process. This innovative multimodal strategy achieves a multitude of related goals. First, we aspire to significantly elevate the visual quality of environmental photos by harnessing the power of deep learning techniques. This will enable a clearer and more insightful examination of numerous environmental elements and events. Second, the integration of spectroscopy into the imaging system, by simultaneously capturing spectrum information and conventional visual data, allows for a more comprehensive understanding of the environmental conditions under study. Thirdly, we aim to streamline data collection procedures, reducing complexity and enhancing efficiency in ecological monitoring and analysis duties by merging spectroscopy and imaging within a single framework. Ultimately, by achieving these ambitious goals, we aim to catalyze the development of novel instruments and research approaches for environmental monitoring and study, with potential applications in disciplines including ecology, climatology, and remote sensing.

II. Literature review

According to [15] Deep-learning-based tomographic imaging is a significant application of artificial intelligence and machine learning, particularly in biomedicine. Since 2016, researchers have been actively researching deep learning techniques for tomographic reconstruction, producing multi-dimensional structures from externally measured data. This emerging field is crucial for personalized, preventive, and precision medicine, making it intelligent, inexpensive, and indiscriminate.[16] reviews the history of remote sensing object detection (RSOD) techniques, including traditional and DL-based methods. It introduces a taxonomy based on various detection methods, focusing on attention mechanisms, multi-scale feature fusion, and super-resolution. The paper also introduces open-source benchmarks and evaluation metrics. The paper concludes by discussing challenges and potential trends in the field of RSOD, providing a reference for researchers new to the field. The development of deep learning technology has significantly improved the performance of RSIs.

In a study by [17] used airborne hyperspectral remote sensing to monitor inland water quality. It uses two deep learning-based regression models to estimate seven optically inactive parameters. The models show superior accuracy, particularly the patch DNNR model, compared to traditional methods. The results provide a new approach for estimating optically inactive parameters. [18] introduces a new extended reality (XR) and deep-learning-based IoMT solution for COVID-19 telemedicine diagnostics. It combines virtual reality/AR remote surgical plan/rehearse hardware, 5G cloud computing, and deep learning algorithms for real-time COVID-19 treatment scheme clues. The system outperforms existing perception techniques and opens new research for IoMT implementation.

The study by [19] presented an end-to-end deep neural network approach (AUTOMAP) for improving image quality in low-field MRI systems. It outperforms contemporary image-based denoising algorithms and suppresses noise-like spike artifacts, demonstrating significant improvements in low-field imaging. [20] The multichannel water body detection network (MC- WBDN) is a novel DCNN model that uses three innovative components: a multichannel fusion module, an Enhanced Atrous Spatial Pyramid Pooling module, and Space-to- Depth/Depth-to- Space operations. Experimental results show the MC-WBDN model outperforms state-of-the-art methods, outperforming other DCNN models, is more robust to light and weather variations, and can better distinguish small water bodies.[21] explores a robot- assisted ultrasonic testing system using track-scan imaging to improve detecting coverage and contrast of curved parts defects. A visual geometry group-UNet (VGG-UNet) deep learning network is proposed to optimize ultrasonic images. The network improves signal-to-noise ratio (PSNR) and structural similarity index measure (SSIM) by 39 dB and 0.99, respectively, and increases the resolution of reconstructed ultrasonic images by approximately 10 times.

III. Methodology

3.1 Data Collection

Data is collected from the Indian Pines dataset using the Airborne Visible/Infrared Imaging Spectrometer (AVIRIS) sensor, which covers the Indian Pines test site in northwestern Indiana. Similarly, the Salinas dataset is collected by the Airborne Imaging Spectrometer (DAIS) sensor, which encompasses the Salinas Valley in California. These datasets provide fundamental resources for hyperspectral image analysis and classification studies in remote sensing applications.

3.2 Data Pre-processing

During the pre-processing phase, the Indian Pines and Salinas datasets are standardized and reshaped to guarantee compatibility with the model. Techniques such as normalization are implemented to standardize data, while augmentation methods like twisting and rotation are implemented to improve the robustness of the model and the diversity of the dataset. Combined, these pre-processing processes optimize the datasets for classification and analysis.

3.3 Train-Test Split

After pre-processing, the dataset is subjected to a train-test split, which typically allocates 80% of the data to the training set and 20% to the testing set. This division guarantees that the model is trained on a suitably extensive portion of the data to identify patterns and relationships, while also supplying an independent subset for evaluating its performance on unseen data. The training set optimises the model's parameters, while the testing set evaluates its capacity to generalize to new samples. To guarantee uniform evaluations across various datasets and experiments, this standardized division ratio is frequently implemented.

3.4 Model Building

This stage involves the model's construction by the Cross-domain Convolutional Neural Network (CNN) architecture. This entails the establishment of input layers that are customized to the dataset's characteristics, the implementation of convolutional layers for feature extraction, the introduction of shared layers to capture domain-independent features, and the addition of dataset- specific classification layers. Optimizing the model's capacity to classify hyperspectral data across various domains is achieved through this methodology.

3.5 Hyperparameter tuning

Following model construction, hyperparameter optimization is the subsequent critical phase, during which the model's performance is further optimized. Systematic adjustments to hyperparameters, including learning rate, sample size, and dropout rate, are implemented to optimize the model's functionality. The purpose of hyperparameter tuning is to identify the most effective configuration for the model, which will optimize its generalization and accuracy. It is possible to efficiently investigate the hyperparameter space by employing methods such as grid or random search. Cross-validation techniques may be employed to assess various hyperparameter configurations and prevent overfitting. The model is prepared for training on the training dataset to further refine its parameters and enhance performance after the optimal hyperparameters have been determined.

3.6 Model Evaluation

The "model evaluation" process examines whether a created model can be applied to new data to establish its generalizability. Accuracy, precision, recall, and F1 score are some of the numerous measures used to assess a models' ability.

3.7 Performance Metrics

Accuracy: The most straightforward way to measure how often the classifier makes correct predictions is by using accuracy. This could also be seen as the ratio of all true positive predictions divided by the total number of predictions made.

$$Accuracy = \frac{TP + TN}{S} \quad (1)$$

Precision: In contrast to this ratio, which presents the percentage of false negatives in addition to one minus from it, i.e., (1—precision), 1/Precision yields recall.

$$\mathrm{Pr}ecision = \frac{TP}{TP + FP} \quad (2)$$

Recall: On the other hand, there are called false negatives in relation to True Negatives.

$$\mathrm{Re}call = \frac{TP}{TP + FN} \quad (3)$$

F1-Score: It is obtained by taking the harmonic mean between recall and precision scores.

$$F1 = \frac{2 * \mathrm{Pr}ecision * \mathrm{Re}call}{\mathrm{Pr}ecision + \mathrm{Re}call} \quad (4)$$

3.8 Tools and Software for Analysis

For our investigation, we extensively used the programming language Python, taking advantage of its vast ecosystem for analyzing deep learning models. In addition, Google Collab served as our main computing platform

IV. RESULTS AND DISCUSSION

Results

In this section, we compare the Cross-domain CNN model to DenseNet and Standard-CNN for hyperspectral image classification. Each model is evaluated using accuracy, precision, recall, and F1-score. We investigate confusion matrices to better understand pixel and non-pixel categorization accuracy. These findings show the Cross-domain CNN's improved hyperspectral image classification ability.

Table IV-1Confusion matrix of Cross-Domain CNN, DenseNet, Standard-CNN

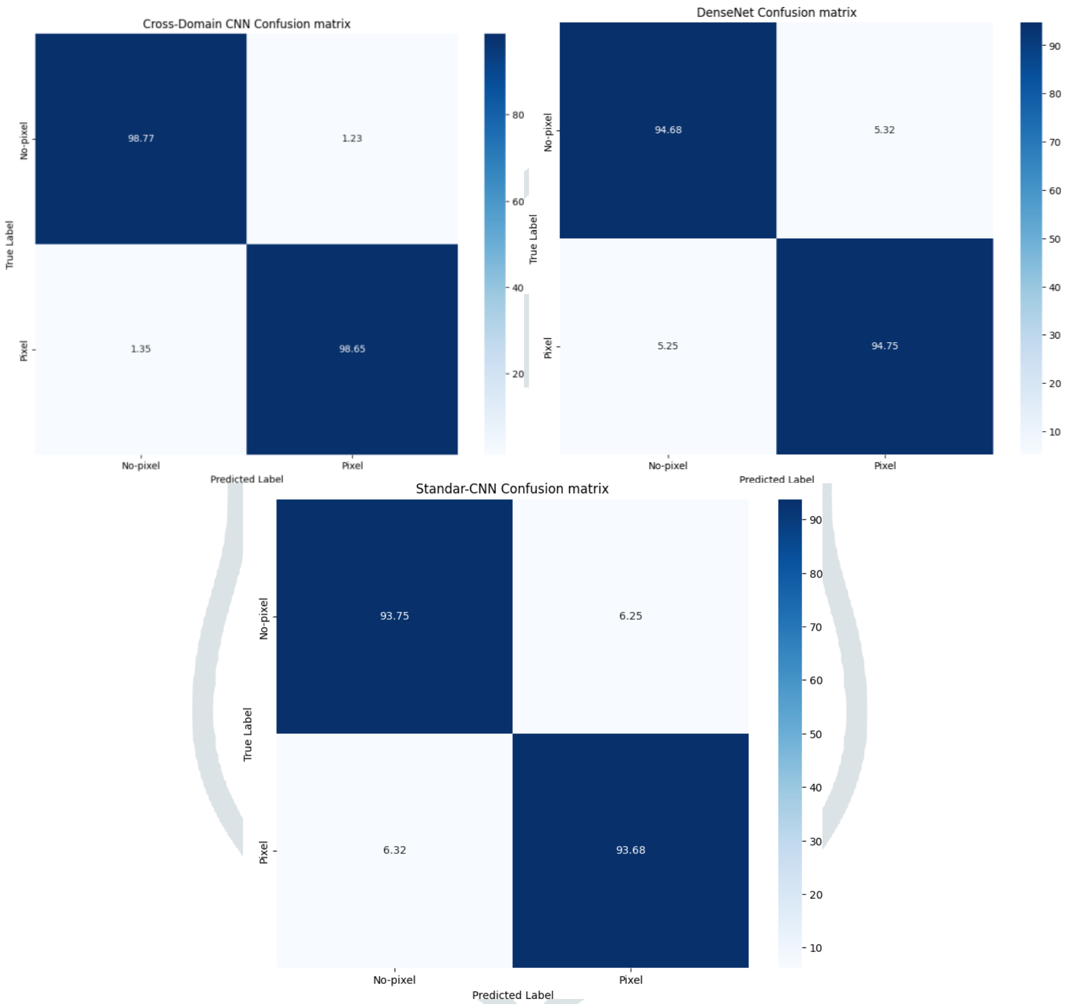

The confusion matrices above can be divided into two categories: pixel and nonpixel. The proposed Cross-domain CNN accurately identified 98.77% of pixels as true positives (TP) and 98.65% of non-pixels as true negatives (TN), with a false positive rate (FP) of 1.23% and false negative rate (FN) of 1.35%. This emphasizes its great accuracy and dependability in hyperspectral picture classification. In comparison, the DenseNet model had a TP rate of 94.6% and a TN rate of 94.75%, but higher error rates of 5.32% FP and 5.25% FN. The Standard-CNN model performed the least successfully, with a TP rate of 93.75% and a TN rate of 93.68%, as well as 6.25% FP and 6.32% FN. These findings clearly show that Cross-domain CNN outperforms DenseNet and Standard-CNN in reliably categorizing pixels and non-pixels in hyperspectral pictures, making it the most dependable model for this application.

Table IV-2Table 2Performance Metrics

Models	**Accuracy**	**Precision**	**Recall**	**F1-Score**
Cross-Domain CNN	0.98714	0.98714	0.98714	0.98714
DenseNet	0.94513	0.94345	0.94534	0.94753
Standard-CNN	0.93713	0.93713	0.93713	0.93713

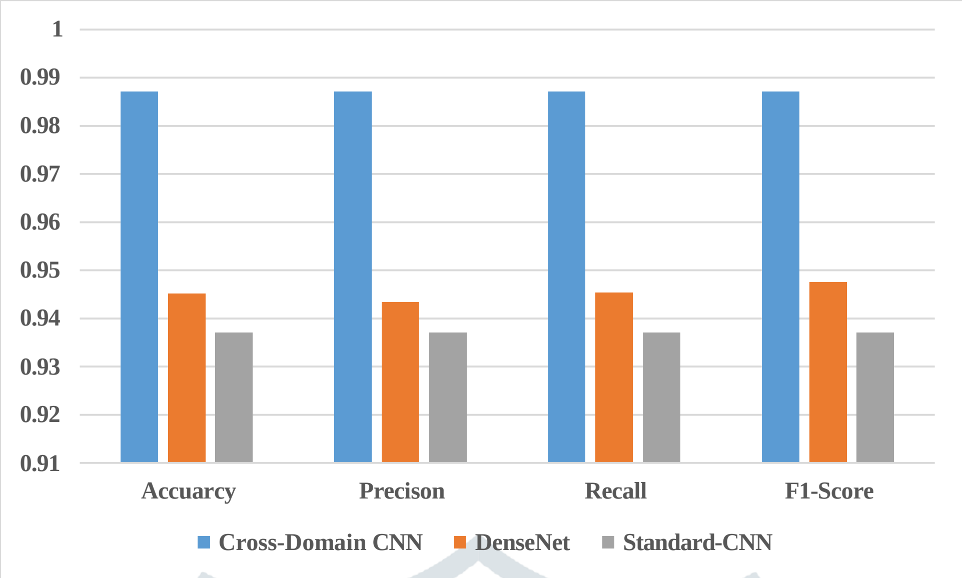

From the above table it is observable that the suggested Cross-domain CNN model performs much better in pixel-wise classification for hyperspectral pictures than DenseNet and Standard-CNN, according to the results. With a 0.98714 accuracy, precision, recall, and F1-score, the Cross- domain CNN demonstrated remarkable and well-balanced performance in all parameters. Standard-CNN demonstrated consistent but poorer performance with all measures at 0.93713, while DenseNet attained an accuracy of 0.94513, with precision, recall, and F1-score around 0.945. These outcomes show that the Cross-domain CNN is more effective than DenseNet and Standard- CNN at generalizing and correctly classifying pixels in hyperspectral imaging tasks

V. Discussion

It is clear that the Cross-domain CNN beats DenseNet and Standard-CNN in hyperspectral picture categorization. The confusion matrices show the Cross-domain CNN's outstanding accuracy, with high true positive rates in both pixel and non-pixel categories, demonstrating that it can efficiently discriminate between classes. In contrast, DenseNet and Standard-CNN have lower true positive rates and larger error rates, indicating less accurate classification performance. The Cross-domain CNN's superiority is further validated by performance measurements that consistently show high accuracy, precision, recall, and F1 score. These findings illustrate the Cross-domain CNN's ability to generalize across varied datasets and effectively categorize hyperspectral pictures, demonstrating its promise as a strong model for complicated remote sensing applications. The results underline the need of specialized models that are customized to the specific properties of hyperspectral data, as well as the need for more study to improve the efficiency and efficacy of hyperspectral image categorization algorithms.

VII. CONCLUSION

Finally, this work evaluated three models for hyperspectral image classification: Cross-domain CNN, DenseNet, and Standard-CNN. The rigorous research of confusion matrices and performance indicators provided clear insights into their individual capacities. The Cross-domain CNN emerges as the best performer, with high accuracy, precision, recall, and F1-score measures. Its capacity to reliably identify pixels and non-pixels in hyperspectral pictures demonstrates its ability to handle such complicated data. DenseNet and Standard-CNN, on the other hand, perform well but fall short of Cross-domain CNN in terms of error rates and classification reliability. These results emphasize the need of using customized models designed expressly for the unique properties of hyperspectral data. Future research should concentrate on improving and enhancing hyperspectral image classification algorithms to address the changing needs of remote sensing applications. By constantly increasing the accuracy and efficiency of these models, we can improve our capacity to extract relevant insights from hyperspectral images and get a better knowledge of numerous environmental processes. Finally, the continuous development of improved hyperspectral image classification systems offers considerable potential for solving real- world problems and fostering innovation in remote sensing and other domains

References

[1] I. Goodfellow, Y. Bengio, and A. Courville, *Deep learning*. MIT press, 2016.
[2] T. Young, D. Hazarika, S. Poria, and E. Cambria, "Recent trends in deep learning based natural language processing," *ieee Comput. Intell. Mag.*, vol. 13, no. 3, pp. 55–75, 2018.
[3] A. Krizhevsky, I. Sutskever, and G. E. Hinton, "ImageNet classification with deep convolutional neural networks," *Commun. ACM*, vol. 60, no. 6, pp. 84–90, 2017.
[4] D. Silver *et al.*, "Mastering the game of go without human knowledge," *Nature*, vol. 550, no. 7676, pp. 354–359, 2017.
[5] W. S. McCulloch and W. Pitts, "A logical calculus of the ideas immanent in nervous activity," *Bull. Math. Biophys.*, vol. 5, pp. 115–133, 1943.
[6] M. SHOLIKAH, "PENENTUAN JALUR TERBAIK MENGGUNAKAN ALGORITMA GLOWWORM SWARM OPTIMIZATION BERDASARKAN DARI HASIL OUTPUT KONDISI KEPADATAN KENDARAAN MENGGUNAKAN 1DCNN."
[7] S. Hochreiter and J. Schmidhuber, "Long Short-Term Memory," *Neural Comput.*, vol. 9, no. 8, pp. 1735–1780, 1997, doi: 10.1162/neco.1997.9.8.1735.
[8] Y. LeCun, L. Bottou, Y. Bengio, and P. Haffner, "Gradient-based learning applied to document recognition," *Proc. IEEE*, vol. 86, no. 11, pp. 2278–2324, 1998.

[9] D. Mazza and M. Pagani, "Automatic differentiation in PCF," *Proc. ACM Program. Lang.*, vol. 5, no. POPL, pp. 1–27, 2021.
[10] Y. Liu *et al.*, "Artificial intelligence–based breast cancer nodal metastasis detection: insights into the black box for pathologists," *Arch. Pathol. Lab. Med.*, vol. 143, no. 7, pp. 859–868, 2019.
[11] C.-Y. Yang, C. Ma, and M.-H. Yang, "Single-image super-resolution: A benchmark," in *Computer Vision–ECCV 2014: 13th European Conference, Zurich, Switzerland, September 6-12, 2014, Proceedings, Part IV 13*, 2014, pp. 372–386.
[12] R. Gräf, J. Rietdorf, and T. Zimmermann, "Live cell spinning disk microscopy," *Microsc. Tech. -/-*, pp. 57–75, 2005.
[13] J. Johnson, A. Alahi, and L. Fei-Fei, "Perceptual losses for real-time style transfer and super-resolution," in *Computer Vision–ECCV 2016: 14th European Conference, Amsterdam, The Netherlands, October 11-14, 2016, Proceedings, Part II 14*, 2016, pp. 694–711.
[14] V. A. Knyaz, V. V Kniaz, and F. Remondino, "Image-to-voxel model translation with conditional adversarial networks," in *Proceedings of the European Conference on Computer Vision (ECCV) Workshops*, 2018, p. 0.
[15] G. Wang, J. C. Ye, and B. De Man, "Deep learning for tomographic image reconstruction," *Nat. Mach. Intell.*, vol. 2, no. 12, pp. 737–748, 2020.
[16] Z. Li *et al.*, "Deep learning-based object detection techniques for remote sensing images: A survey," *Remote Sens.*, vol. 14, no. 10, p. 2385, 2022.
[17] C. Niu, K. Tan, X. Jia, and X. Wang, "Deep learning based regression for optically inactive inland water quality parameter estimation using airborne hyperspectral imagery," *Environ. Pollut.*, vol. 286, p. 117534, 2021.
[18] Y. Tai, B. Gao, Q. Li, Z. Yu, C. Zhu, and V. Chang, "Trustworthy and intelligent covid-19 diagnostic iomt through xr and deep-learning-based clinic data access," *IEEE Internet Things J.*, vol. 8, no. 21, pp. 15965–15976, 2021.
[19] N. Koonjoo, B. Zhu, G. C. Bagnall, D. Bhutto, and M. S. Rosen, "Boosting the signal-to-noise of low-field MRI with deep learning image reconstruction," *Sci. Rep.*, vol. 11, no. 1, p. 8248, 2021.
[20] K. Yuan, X. Zhuang, G. Schaefer, J. Feng, L. Guan, and H. Fang, "Deep-learning-based multispectral satellite image segmentation for water body detection," *IEEE J. Sel. Top. Appl. Earth Obs. Remote Sens.*, vol. 14, pp. 7422–7434, 2021.
[21] Y. Mei, H. Jin, B. Yu, E. Wu, and K. Yang, "Visual geometry group-UNet: deep learning ultrasonic image reconstruction for curved parts," *J. Acoust. Soc. Am.*, vol. 149, no. 5, pp. 2997–3009, 2021.